complexes are five-coordinate with no ligands *trans* to the μ-oxo system.) The two Fe–N contacts of intermediate length appear to be a consequence of accommodating the longest contact.

It is concluded that the conformation of the cation is well established and that there are indications of a variation in Fe–N distance with position in the tetraethylenepentaamine chain, but that further discussion of the details of the cation dimensions would not be justified on the basis of this analysis alone.

We thank the S.R.C. for financial assistance.

References

COGGON, P., MCPHAIL, A. T., MABBS, F. E. & MCLACHLAN, V. N. (1971). *J. Chem. Soc.* (*A*), pp. 1014–1019.
GERLOCH, M., MCKENZIE, E. D. & TOWL, A. D. C. (1969). *J. Chem. Soc.* (*A*), pp. 2850–2858.
HAMILTON, W. C. (1965). *Acta Cryst.* **18**, 502–510
HOUSE, D. A. & GARNER, C. S. (1966). *Inorg. Chem.* **5**, 2097–2103.
LIPPARD, S. J., SCHUGAR, H. & WALLING, C. (1967). *Inorg. Chem.* **6**, 1825–1831.
MELBY, L. R. (1970). *Inorg. Chem.* **9**, 2186–2188.
ROLLETT, J. S. (1969). In *Crystallographic Computing*, edited by F. R. AHMED, pp. 169–172. Copenhagen: Munksgaard.
ROLLETT, J. S. & CARRUTHERS, J. R. (1975). To be published.
SARGESON, A. M. & SEARLE, G. H. (1965). *Inorg. Chem.* **4**, 45–52.
SNOW, M. R. (1972*a*). *J. Chem. Soc. Dalton*, pp. 1627–1634.
SNOW, M. R. (1972*b*). *J. Amer. Chem. Soc.* **92**, 3610–3617.
SNOW, M. R., BUCKINGHAM, D. A., MARZILLI, P. A. & SARGESON, A. M. (1969). *Chem. Comm.* pp. 891–892.
WASER, J. (1963). *Acta Cryst.* **16**, 1091–1094.
WATSON, H. C., SHOTTON, D. M., COX, J. M. & MUIRHEAD, H. (1970). *Nature, Lond.* **225**, 805–811.

Acta Cryst. (1975). B**31**, 1442

Electron Microscopy of the Perovskite Polytypes $Ba_4Ta_3LiO_{12}$ and $Ba_5W_3Li_2O_{15}$

BY J. L. HUTCHISON AND A. J. JACOBSON

Inorganic Chemistry Laboratory, South Parks Road, Oxford OX1 3QR, England

(*Received* 15 *January* 1975; *accepted* 17 *January* 1975)

High-resolution lattice images have been obtained for the ordered perovskite polytypes $Ba_5W_3Li_2O_{15}$ (*cccch*) and $Ba_4Ta_3LiO_{12}$ (*ccch*). The lattice images can be correlated with the stacking sequence of the BaO_3 layers and, for $Ba_5W_3Li_2O_{15}$, with the presence of the ordered arrangement of corner-sharing LiO_6 octahedra.

Introduction

The study of structural imperfections in complex oxides by high-resolution electron microscopy has received much attention in recent years. In particular, the ability of an electron microscope to generate from a thin crystal an image which closely resembles the projected structure of that crystal has led to new insights into the ultramicro-structure of complex oxides. The niobium oxide 'block' structures and a variety of 'crystallographic shear' structures have been successfully examined in this way. The structures consist of relatively open networks of corner-sharing $[MO_6]$ octahedra, with centre to centre distances of 0·38 nm, comparable to the resolving power of the electron microscope. The networks are nominally one octahedron deep, and lattice images of crystals oriented with this axis parallel to the electron beam may be correlated with the actual structure in terms of dark contrast indicating areas of high projected charge density. The interpretation was possible at resolutions of 0·5–0·8 nm (Allpress, 1970; Hutchison & Anderson, 1972), although micrographs obtained at a resolution of about 0·4 nm (Iijima, 1971) were more convincing. These experimental observations which provide an empirical interpretation of image contrast have been recently confirmed by *n*-beam image calculations (O'Keefe, 1973). Much of the success of these studies of niobium oxides relies on the fact that the projected charge density, along (010), reveals channels between corner-shared octahedra, and Allpress & Sanders (1973) have suggested that other suitable systems would require such voids in projections.

In more closely packed systems, where the projected charge density is less simple, calculations have not yet been made, and only a few systems have been examined experimentally (McConnell, Hutchison & Anderson, 1974). In this work we have investigated the correlation between lattice images and crystal structure for two ordered perovskite polytypes. ABO_3 compounds of the perovskite type can be described in terms of AO_3 close-packed layers, with B cations in the O_6 octahedra. Many polytypes are known which differ in the ratio of the number of cubic to hexagonal stacked layers [for examples see Goodenough & Longo (1970)]. The two compounds chosen for study were eight-layer

$Ba_4Ta_3LiO_{12}$ and ten-layer $Ba_5W_3Li_2O_{15}$. The preparations and structures of these materials have recently been reported (Negas, Roth, Parker & Brower, 1973; Collins, Jacobson & Fender, 1974; Jacobson, Collins & Fender, 1974; Jendrek, Potoff & Katz, 1974).

Eight-layer $Ba_4Ta_3LiO_{12}$ has a stacking sequence which may be described as (*ccch*), or |(4)|(4)| in Zhdanov notation (see *International Tables for X-ray Crystallography*). The lattice parameters are $a=0{\cdot}5798$, $c=1{\cdot}906$ nm. In this structure (Fig. 1) the pair of face-shared octahedra are occupied by equal amounts of Ta and Li probably randomly distributed; the corner-shared octahedra contain only Ta.

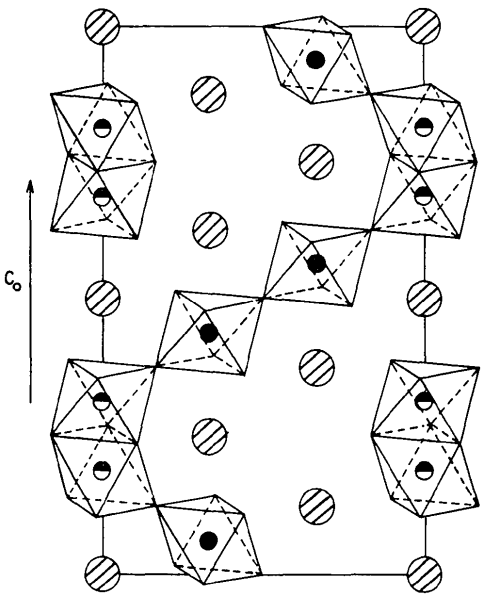

Fig. 1. Structure of $Ba_5W_3Li_2O_{15}$. Hatched circles: Ba; filled circles: W; half-filled circles: W, Li; open circles: Li.

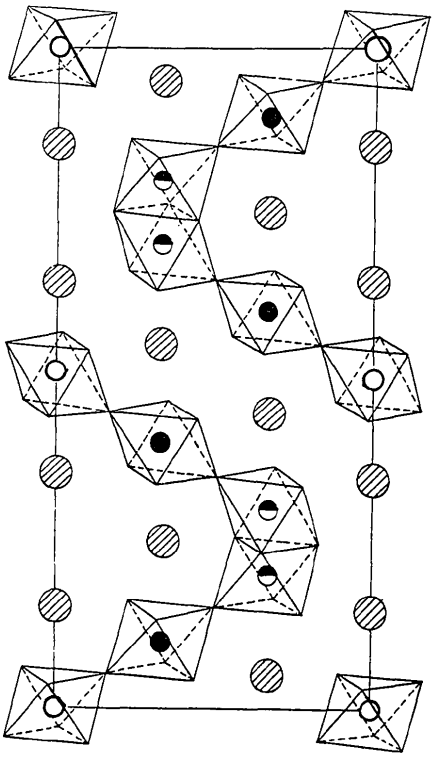

Fig. 2. Structure of $Ba_4Ta_3LiO_{12}$. Filled circles: Ta.

In the ten-layer material $Ba_5W_3Li_2O_{15}$, the stacking sequence is (*cccch*) or |(5)|(5)|. The lattice parameters are $a=0{\cdot}5756$, $c=2{\cdot}372$ nm. The structure is shown in Fig. 2. The face-shared octahedra are occupied by equal amounts of W and Li, and the remaining two W and one Li are ordered over the octahedra which share only corners, in the sequence W–Li–W.

Both structures have the space group $P6_3/mmc$, and layer separations of close to 0·24 nm.

Experimental

Lattice images which can be related directly to structure at near atomic level, so called 'structure images', are obtained only under certain closely defined conditions. The specimen crystal must be sufficiently thin (≤ 10 nm) to behave essentially as a phase object and it must be aligned with the chosen axis of projection parallel (within 10^{-3} rad) to the electron beam (Cowley & Iijima, 1972). In addition structure images require underfocusing of the objective lens in order to compensate for spherical aberration (Scherzer, 1949), which retards the phases of diffracted beams. This defocus value is typically of the order of 50–60 nm, and is determined by the objective lens characteristics.

An objective aperture which eliminates most widely scattered beams is necessary to control spherical aberration further although additional contrast may arise as a result from Fourier series truncation effects [see for example Sanders & O'Keefe (1974)].

In the present study a Siemens Elmiskop 102 electron microscope was used with an accelerating voltage of 125 keV. Thin crystals on carbon-coated Cu grids were oriented by means of a $\pm 45°$ double tilt cartridge. Images were obtained at magnifications of 500000× with a 50μ objective aperture which includes diffracted beams out to about 3 nm^{-1}.

Results and discussion

$Ba_5W_3Li_2O_{15}$

It is useful to recognize two features of the structure of $Ba_5W_3Li_2O_{15}$ (see Fig. 2) in interpreting the lattice images: (i) the mirror plane at a hexagonal close-packed layer reverses the slope of both the corner-linked octahedra and the rows of Ba atoms, (ii) the central of the string of three corner-shared octahedra contains only Li, which has a low electron scattering power. Thus the Li-filled layers of octahedra are effectively 'electron transparent' layers in the crystal and ought intuitively to give rise to white contrast in an optimally focused image.

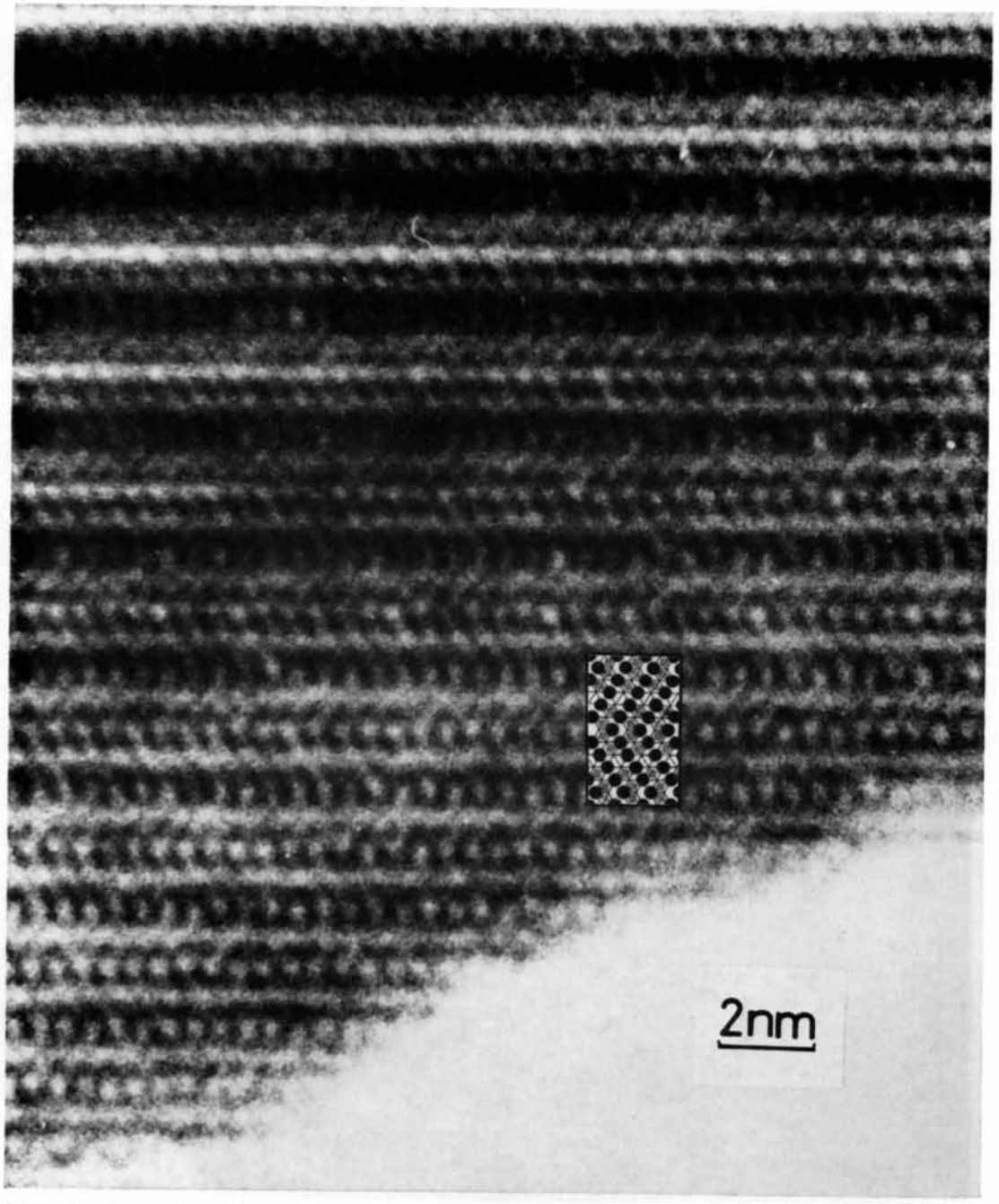

Fig. 3. [10$\bar{1}$0] lattice image of $Ba_5W_3Li_2O_{15}$. Inset: idealized projection showing Ba atoms (filled circles) and Li-filled octahedra (unshaded parallelograms).

[*To face p.* 1444

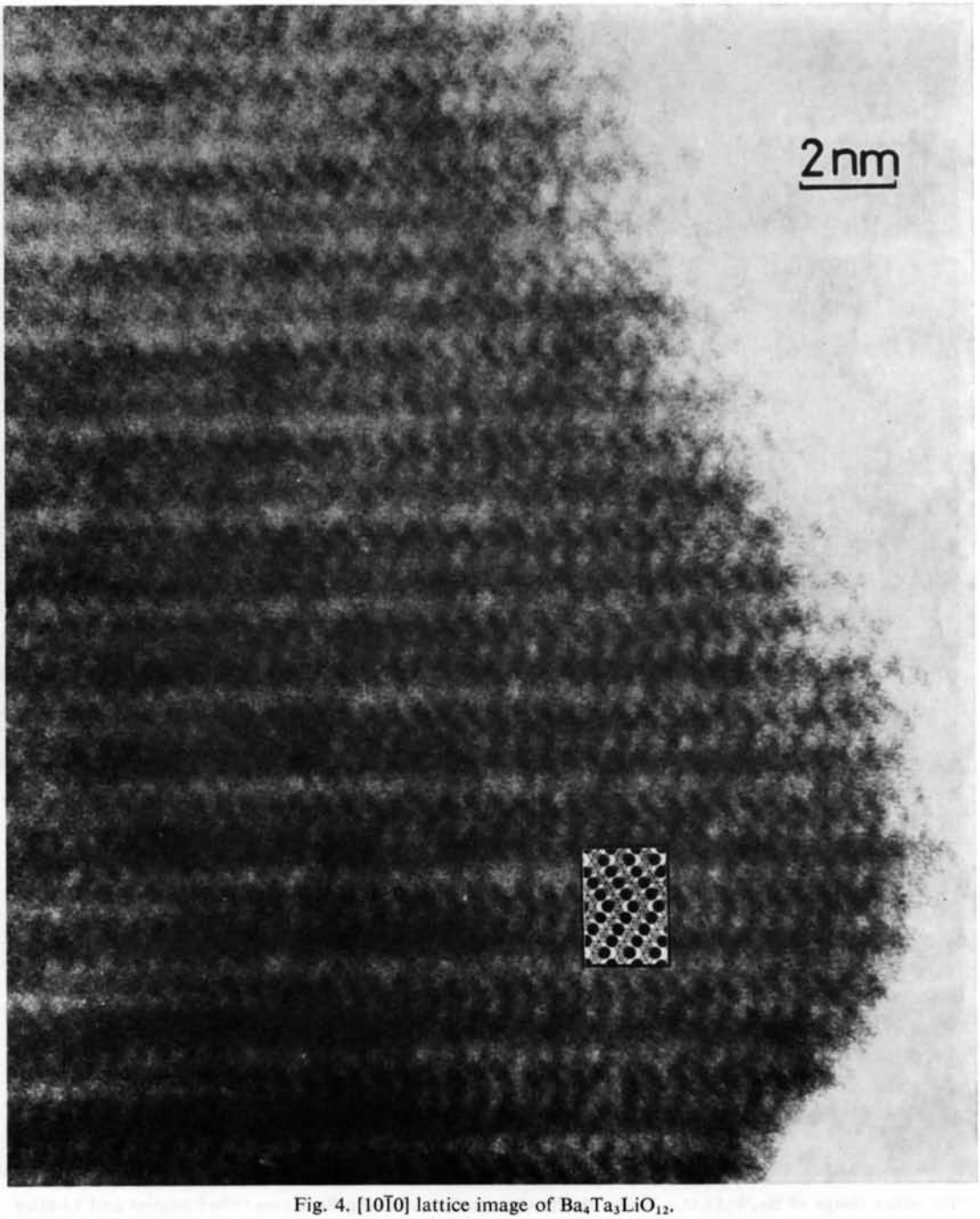

Fig. 4. [10$\bar{1}$0] lattice image of $Ba_4Ta_3LiO_{12}$.

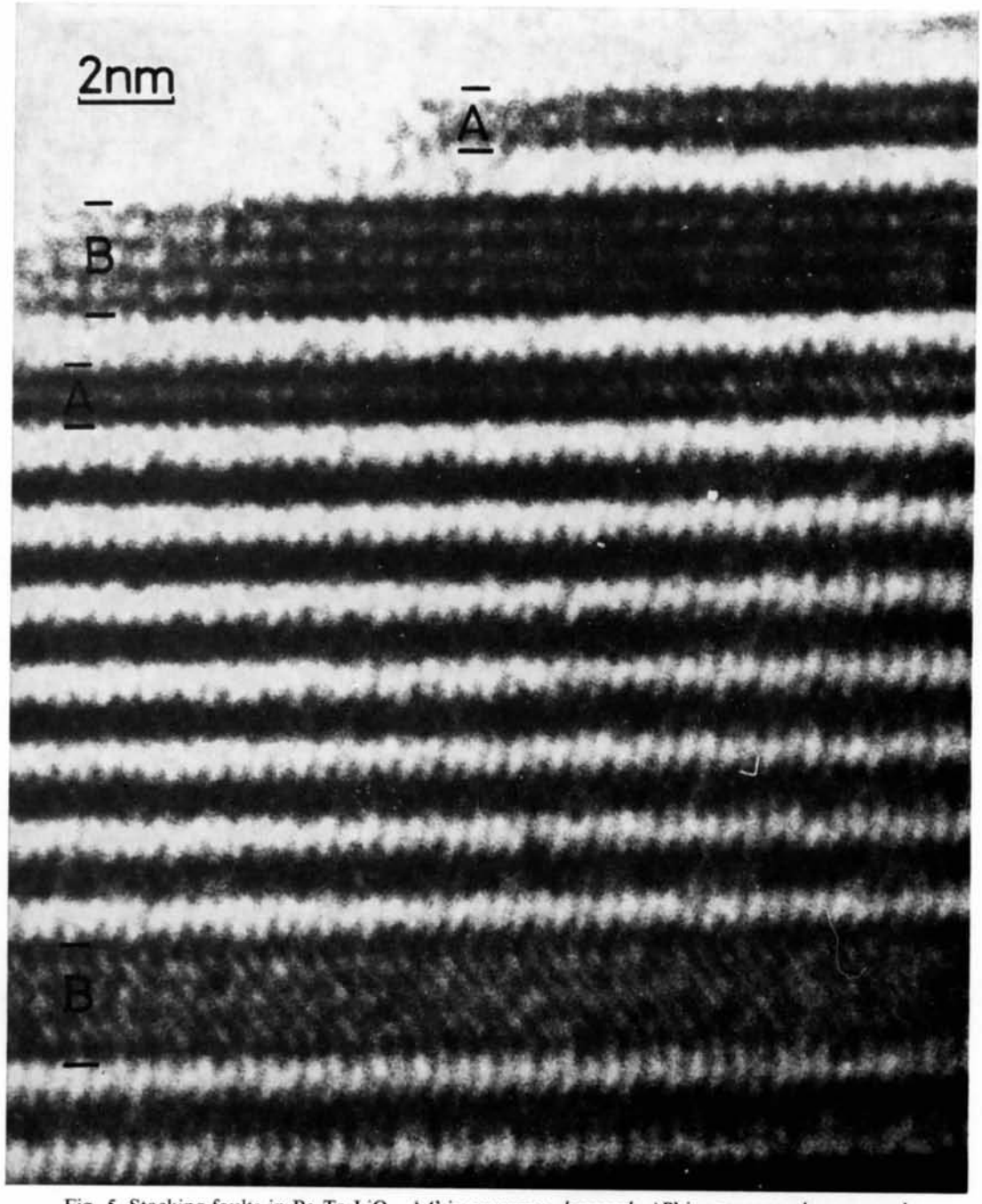

Fig. 5. Stacking faults in $Ba_4Ta_3LiO_{12}$. '*A*' is sequence –*hccccch*– '*B*' is sequence –*hcccccccch*–.

Fig. 3 is a lattice image of $Ba_5W_3Li_2O_{15}$ with $[10\bar{1}0]$ parallel to the electron beam. It is selected from a series of micrographs taken over a range of defocus values from $\Delta f \simeq 0$ to about 100 nm. Within this range the optimum defocus determined by the periodicity of the structure and the lens aberrations occurs at about 50–60 nm. In Fig. 3 the mirror planes 1·18 nm apart are visible and the ordered Li layers display white line contrast. The lattice image may be compared with the inset of the idealized structure in the same orientation. In the thinnest region of the crystal, chevrons corresponding to the columns of Ba atoms and WO_6 octahedra alternating in direction every five layers can be seen. As the crystal becomes thicker the true periodicity of the structure, 2·37 nm, becomes dominant and the horizontal white lines can no longer be correlated with the ordered Li layers. No stacking faults were observed in the crystals examined, indicating that a high degree of ordering had been achieved.

$Ba_4Ta_3LiO_{12}$

The eight-layer polytype $Ba_4Ta_3LiO_{12}$ has a mirror plane at the hexagonal layer, as in the W compound, but the ordered Li-filled layers are absent. Consequently the contrast would be expected to be similar, but without the white Li lines. Fig. 4 is a lattice image of $Ba_4Ta_3LiO_{12}$ with the idealized structure in the same orientation inset. The image shows an array of chevrons which, as before, we interpret as being planes of Ba atoms viewed edge on. Slight differences in focus between the two micrographs (Figs. 3 and 4) give rise to contrast features which, although mutually consistent, are not identical.

Despite long annealing times at high temperature in this sample preparation, the material contained a number of defects in the form of stacking faults. Fig. 5 shows an image taken with the crystal set about 2° from the exact $[10\bar{1}0]$ orientation. In this way successive elements of twin-related structure (successive *ccc*-sequences) display opposite contrast, and stacking faults are strikingly revealed although it is impossible to correlate fine details. In Fig. 5 the defects '*A*' correspond to a layer sequence *ccccch* and defects '*B*' are of the sequence *ccccccccch*.

Conclusions

A direct correlation between the stacking sequence of BaO_3 layers and the high resolution lattice images is possible for the two perovskite polytypes $Ba_5W_3Li_2O_{15}$ and $Ba_4Ta_3LiO_{12}$. Confirmation of the interpretation is found in the appearance of contrast which may be associated with the presence of layers of effectively 'electron transparent' LiO_6 octahedra in the W compound.

$Ba_5W_3Li_2O_{15}$ shows no evidence for the presence of stacking faults whereas several regions of perfect cubic stacking were found in $Ba_4Ta_3LiO_{12}$. This is consistent with observations made during the sample preparations. In the W compound, ordering was detected as the reaction progressed whereas a disordered cubic phase was initially formed at 1000°C for the Ta material and further prolonged annealing at 1300°C was required to obtain the eight-layer polytype.

The results suggest that the determination by electron microscopy of unknown complex stacking sequences in perovskite polytypes is feasible. However, because the lattice images formed are sensitive to the defocus of the objective lens, in complex unknown structures the choice of the optimum defocus may not be straightforward. It is clearly desirable therefore to combine further experimental work with an extension of lattice image calculations to these more densely packed structures.

References

ALLPRESS, J. G. (1970). *J. Solid State Chem.* **2**, 78–93.

ALLPRESS, J. G. & SANDERS, J. V. (1973). *J. Appl. Cryst.* **6**, 165–190.

COLLINS, B. M., JACOBSON, A. J. & FENDER, B. E. F. (1974). *J. Solid State Chem.* **10**, 29–35.

COWLEY, J. M. & IIJIMA, S. (1972). *Z. Naturforsch.* **27a**, 445–451.

GOODENOUGH, J. B. & LONGO, J. M. (1970). *Crystallographic and Magnetic Properties of Perovskite and Perovskite Related Compounds.* Landolt-Börnstein, New Series, Group III, Vol. 4*a*. New York: Springer-Verlag.

HUTCHISON, J. L. & ANDERSON, J. S. (1972). *Phys. Stat. Sol.* (*a*), **9**, 207–213.

IIJIMA, S. (1971). *J. Appl. Phys.* **42**, 5891–5893.

JACOBSON, A. J., COLLINS, B. M. & FENDER, B. E. F. (1974). *Acta Cryst.* B**30**, 816–819.

JENDREK, E. F., POTOFF, A. D. & KATZ, L. (1974). *J. Solid State Chem.* **9**, 375–379.

MCCONNELL, J. D. M., HUTCHISON, J. L. & ANDERSON, J. S. (1974). *Proc. Roy. Soc.* A**339**, 1–12.

NEGAS, T., ROTH, R. S., PARKER, H. S. & BROWER, W. S. (1973). *J. Solid State Chem.* **8**, 1–13.

O'KEEFE, M. A. (1973). *Acta Cryst.* A**29**, 389–401.

SANDERS, J. V. & O'KEEFE, M. A. (1974). Proc. 8th International Conference on Electron Microscopy (Canberra).

SCHERZER, O. (1949) *J. Appl. Phys.* **20**, 20–29.